Fundus Camera-Delivered Light-Induced Retinal Degeneration in Mice With the *RPE65* Leu450Met Variant is Associated With Oxidative Stress and Apoptosis

Xin Zhong,[*] Bogale Aredo, Yi Ding, Kaiyan Zhang,[†] Cynthia X. Zhao, and Rafael L. Ufret-Vincenty

Department of Ophthalmology, University of Texas Southwestern Medical Center, Dallas, Texas, United States

Correspondence: Rafael L. Ufret-Vincenty, Department of Ophthalmology, UT Southwestern Medical Center, 5323 Harry Hines Boulevard, Dallas TX 75390-9057, USA;
Rafael.Ufret-Vincenty@UTSouthwestern.edu.

XZ and BA contributed equally to the work presented here and should therefore be regarded as equivalent authors.

Current affiliation: *Department of Ophthalmology, The First Affiliated Hospital of Guangxi Medical University, Nanning, Guangxi, 530021, P. R. China
†Department of Ophthalmology, Hainan Provincial People's Hospital, Haikou, Hainan 570203, P. R. China

Submitted: May 20, 2016
Accepted: September 8, 2016

Citation: Zhong X, Aredo B, Ding Y, Zhang K, Zhao CX, Ufret-Vincenty RL. Fundus camera-delivered light-induced retinal degeneration in mice with the *RPE65* Leu450Met variant is associated with oxidative stress and apoptosis. *Invest Ophthalmol Vis Sci*. 2016;57:5558–5567. DOI:10.1167/iovs.16-19965

Purpose. Oxidative stress, partly due to light, has an important role in many retinal diseases, including macular degeneration and retinal dystrophies. The Leu450Met variant of *RPE65* is expressed in C57BL/6 and in many genetically modified mice. It confers significant resistance to light induced retinal degeneration (LIRD). Our goal was to develop an effective and efficient method to induce LIRD in resistant mice that would recapitulate mechanisms seen in known models of LIRD.

Methods. The retinas of C57BL/6J mice were exposed to light using a murine fundus camera. Two protocols (with and without intraperitoneal fluorescein) were used. Optical coherence tomography (OCT) helped determine the location and extent of retinal damage. Histology, TUNEL assay, quantitative (q) PCR, and immunohistochemistry were performed.

Results. Both protocols consistently generated LIRD in C57BL/6J mice. Optical coherence tomography and histology demonstrated that retinal damage starts at the level of the photoreceptor/outer retina and is more prominent in the superior retina. Fundus camera-delivered light-induced retinal degeneration (FCD-LIRD) is associated with apoptosis, subretinal microglia/macrophages, increased expression of oxidative stress response genes, and C3d deposition.

Conclusions. We characterize two new models of light-induced retinal degeneration that are effective in C57BL/6J mice, and can be modulated in terms of severity. We expect FCD-LIRD to be useful in exploring mechanisms of LIRD in resistant mice, which will be important in increasing our understanding of the retinal response to light damage and oxidative stress.

Keywords: oxidative stress, light damage, *RPE65*, retinal degeneration, Leu450Met

Oxidative stress has an important role in many retinal diseases, including age-related macular degeneration (AMD)[1–8] and retinal dystrophies.[9–11] Due to the combination of high levels of light absorption, oxygen, and oxidizable lipids in the retina, light exposure is a significant contributor to oxidative stress in the retina. Although it is not possible to accurately measure light exposure in humans over decades, there is evidence for an association between light and retinal pathology in AMD and retinal dystrophies.[12–15] Experimental light-induced retinal degeneration (LIRD), particularly in murine models, has been useful in studying mechanisms of disease in the retina, including demonstrating the importance of oxidative stress, apoptosis, complement activation, and inflammation.[16–22] Some of the advantages of LIRD models include the synchronization of the induced cell death, speed of the process, and ability to control the severity of the degeneration.[16] All of these characteristics facilitate the study of the mechanisms involved in retinal degeneration.

However, most LIRD experiments so far have been done in rats and albino mice, which are very susceptible to light-induced retinal damage. C57BL/6 mice have been found to be highly resistant to light injury due in large measure to a variant in *RPE65* (Leu450Met), which slows the regeneration of rhodopsin after photo-bleaching.[23,24] Importantly, a very large number of genetically modified mice are on a C57BL/6 background, making it difficult to test the influence of these genes in the pathophysiology of light-induced retinal degeneration. Finally, it is clear that the human retina is much more resistant to light damage than the retina of albino mice and rats. In fact, while exposure of nonanesthetized Balb/c mice to 5000 lux for 1 hour will cause severe photoreceptor degeneration,[25] the normal light level we humans are exposed to in a sunny day is 10,000 to 20,000 lux even in an area of shade. Since the molecular mechanisms of cell death and of oxidative stress response may vary in the setting of a higher resistance to light damage, we believe that studying LIRD in resistant mice is relevant.

Investigative Ophthalmology & Visual Science

We presented new models of light-induced retinal degeneration that are effective in C57BL/6 mice. Furthermore, we demonstrated that these models cause retinal degeneration that can be modulated in terms of severity. The models are based on delivering light via a mouse retinal imaging system either in the absence or presence of systemic fluorescein. We described the changes in the retina observed with different levels of injury using optical coherence tomography (OCT) and histology. Interestingly, the light damage triggers gene expression and protein changes consistent with an oxidative stress response. We also observed increased photoreceptor cell apoptosis and RPE cell damage.

Methods

Animals and Genotyping of Mice

Animals were handled in accordance with the ARVO Statement for the Use of Animals in Ophthalmic and Vision Research. All procedures were approved by the UT Southwestern Medical Center (UTSW) Institutional Animal Care and Use Committee (Protocol # 2009-0352). Six- to 12-week-old C57BL/6J mice ("B6J"; Jackson Laboratory, Bar Harbor, ME, USA) were used. They were confirmed to be Crb1 wt/wt.[26,27] Mice were acclimated to our animal facility for at least 1 week before being used for experiments. Mice were bred and kept in a barrier animal facility at UTSW under normal lighting conditions with 12-hour-on/12-hour-off cycles. Before performing all procedures, mice were anesthetized with a ketamine-xylazine cocktail (100–5 mg/kg) one at a time. Mouse eyes were dilated using one drop per eye of tropicamide 1% solution (Alcon Laboratories, Inc., Fort Worth, TX, USA) and phenylephrine hydrochloride 2.5% solution (Alcon, Inc., Lake Forest, IL, USA).

Fundus Photography

Fundus photographs of mice were obtained using a Micron IV mouse fundus camera (Phoenix Research Laboratories, Pleasanton, CA, USA) as described previously.[28]

Mouse Setup in Preparation for Light Exposure

Light intensity from the Micron IV mouse fundus camera was measured using a light meter (Cat # S90199; Fisher Scientific, Hampton, NH, USA) to ensure that equal illumination was provided to all eyes. After anesthesia, the mouse was placed on the Phoenix Research Labs mouse stage. Manipulating the stage allowed us to place the mouse eye directly facing the camera lens and approximately centered. A drop of GenTeal gel was applied to cover the surface of the eye. The initial distance from the camera lens to the cornea was 1 to 1.5 cm. The mouse was slowly brought closer to the lens using the stage controls and the camera control, while keeping the cornea at the center of the image, and keeping the focus on the cornea. Before the cornea and the camera lens touched, the optic nerve became visible in the image. A slight adjustment of the stage allowed the operator to overlap the corneal light reflex with the optic nerve image. The camera then was moved to contact the cornea. The optic nerve then was at the center of the fundus image, and the camera was focused on the RPE or retina as needed.

Light Injury

Following overnight dark adaptation, each mouse was anesthetized and the pupils dilated. The eye was centered as described above. For the "Light-only" model of light injury, the Micron IV fundus camera was sharply focused on the RPE layer and light was applied to the retina at an intensity of 125,000 lux (125 K lux; maximum intensity generated by the Micron IV camera after Phoenix Research Laboratories kindly agreed to remove a hardware aperture-lowering piece that is meant to reduce the light output) for a one time exposure of 30 minutes. The image was monitored to ensure that focus and centration were maintained during the entire application time. For the fluorescein-assisted models, fluorescein was administered as a single intraperitoneal injection of either 100 μl of a 1:5 dilution of commercially available 10% fluorescein solution (total dose of 2 mg fluorescein), or 100 μl of a 1:10 dilution (1 mg). Light then was applied at an intensity of 54,000 lux (54 K lux) for 4 minutes. This 54 K lux intensity was used because it was the maximum intensity generated by the Micron IV camera before it was modified. Since we obtained strong, reproducible changes in the retina using this intensity, we continued to use it even after the modification to the Micron IV was made. The illumination was started either 3 minutes after the fluorescein injection (Fl-4@3), or 10 minutes after the injection (Fl-4@10). Mice were kept under normal lighting conditions after the procedure.

OCT Imaging

Mice were anesthetized and pupils were dilated. GenTeal liquid gel (Novartis, East Hanover, NJ, USA) was applied to the corneal surface. Optical coherence tomography images were taken using an image-guided tomographer (Micron IV-OCT2; Phoenix Research Laboratories). For the quantitative assessment of the outer retina reflectivity we used the Freehand tool in ImageJ (http://imagej.nih.gov/ij/; provided in the public domain by the National Institutes of Health, Bethesda, MD, USA) to delineate the ellipsoid zone and the outer segment band in OCT images, and determine their mean intensity. Finally the ratio of the mean intensity of the outer segments to the mean intensity of the outer segements (OS) to the ellipsoid zone was graphed (MI os/MI ellipsoid).

Histology, TUNEL, and Immunohistochemistry

Mouse eyes were enucleated and immediately snap frozen, freeze-substituted, and paraffin-embedded as described previously.[29] Sections (5 μm) through the optic nerve head (ONH) from superior to inferior were used for hematoxylin and eosin (H&E) staining, TUNEL assay, and immunohistochemistry (IHC). For TUNEL and IHC analyses the sections were deparaffinized and rehydrated in a series of xylene and decreasing concentrations of ethanol (KOPTEC 200 proof pure ethanol, CAT # 64-17-5). Sections then were blocked, and stained with either TUNEL mixture or different antibodies (Supplementary Table S1).

ONL Thickness Measurement

Images of the H&E sections were taken at ×20 magnification on either side of the ONH using a Leica DM2000 Upright Compound microscope (Leica Microsystems, Wetzlar, Germany) equipped with an Optronics Microfire color CCD camera (Optronics, Goleta, CA, USA). The H&E images were opened in ImageJ and the ONL thickness was measured at 100 μm intervals starting from the ONH and up to a distance of 1100 μm on each side.

RNA Isolation From Posterior Eye Cups

After anesthesia, enucleation, and removal of the anterior segment, the posterior eye cup was rinsed in 1 × PBS. RNA was

Investigative Ophthalmology & Visual Science

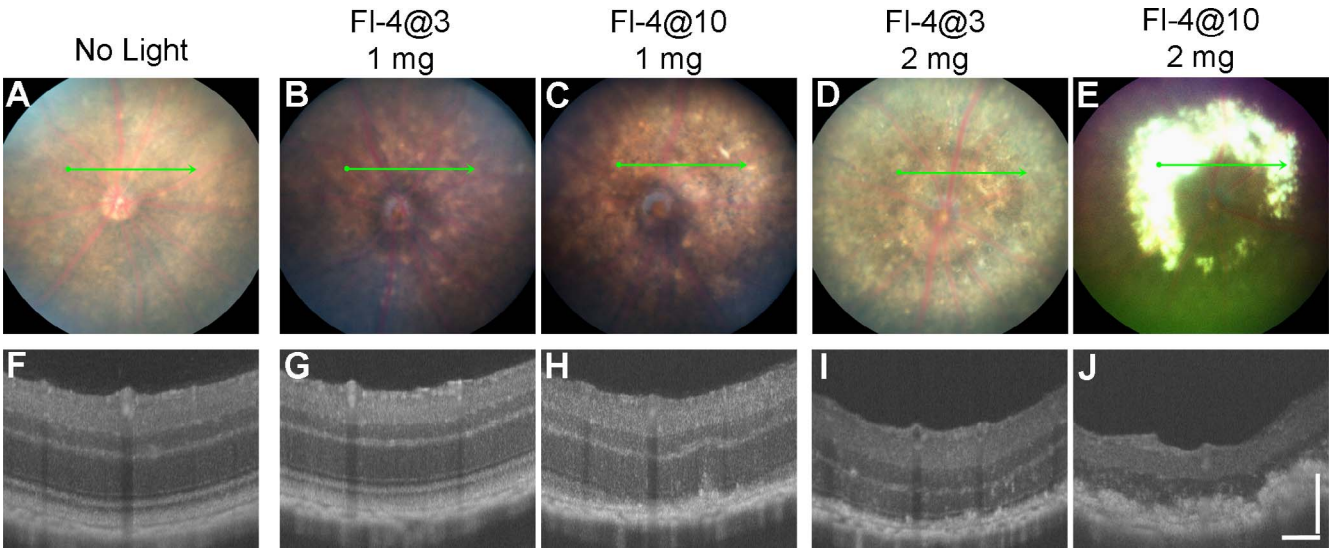

Figure 1. Fundus photographs and OCT images obtained 10 days after mouse eyes were exposed to different doses of intraperitoneal fluorescein (Fl) and to fundus light: (**A**) and (**F**). No light exposure, (**B**) and (**G**). Intraperitoneal fluorescein (1 mg) and 4 minutes of 54 K lux starting 3 minutes after the injection (Fl-4@3 – 1 mg), (**C**) and (**H**). Intraperitoneal fluorescein (1 mg) and 4 minutes of 54 K lux starting 10 minutes after the injection (Fl-4@10 - 1mg), (**D**) and (**I**). Intraperitoneal fluorescein (2 mg) and 4 minutes of 54 K lux starting 3 minutes after the injection (Fl-4@3 - 2mg), (**E**) and (**J**). Intraperitoneal fluorescein (2 mg) and 4 minutes of 54 K lux starting 10 minutes after the injection (Fl-4@10 - 2mg). *Optical coherence tomography scale bars*: 100 μm for *vertical* and *horizontal bars*.

immediately isolated using the miRNeasy Mini Kit (Cat # 217004; Qiagen, Hilden, Germany). In brief, 1 ml of QIAzol Lysis Reagent (Cat # 79306; Qiagen) was added to individual posterior eye cups in 1.5 ml centrifuge tubes and the samples were homogenized with a Bio-Gen PRO200 Homogenizer (PRO Scientific, Inc., Oxford, CT, USA). After adding 200 μl of chloroform (Cat # C2432; Sigma-Aldrich Corp., St. Louis, MO, USA), the tubes were shaken by hand for 15 seconds. After 2 minutes, the samples were transferred to a Phaselock Gel tube (Cat # 2302830; 5 PRIME, Hilden, Germany) and centrifuged for 15 minutes at 18,500*g*. The supernatant was transferred to a new tube, and 100% ethanol (1:1 volume) was added. The entire sample was transferred to an RNeasy Mini Spin Column and processed according to the Qiagen protocol (Cat# 217004; Qiagen). The RNA was eluted with RNase-free water. The RNA quality was checked using an Agilent bioanalyzer and samples with an RNA integrity number (RIN) of above 9 were used for further testing.

Real-Time Quantitative RT-PCR (qPCR)

Genes for qPCR testing (Supplementary Table S2) were chosen based on a pilot screen (data not shown) on a RT^2 Profiler PCR Array for Mouse Oxidative Stress and Antioxidant Defense (Cat # 330111; Qiagen). For qPCR testing, 2 μg RNA were first reverse transcribed using the High Capacity cDNA Reverse Transcription Kit (ABi Part No. 4368814) for qPCR. The iTaq Universal SYBR Green Supermix (Cat # 172-5121; Bio-Rad Laboratories, Hercules, CA, USA) then was used in the qPCR reaction with 4 ng cDNA per well. Singlet qPCR reactions were run in triplicate in the ABi QuantStudio 6 Flex (Thermo Fisher Scientific, Carlsbad, CA, USA) Real-Time PCR machine at 50°C for 2 minutes, 95°C for 10 minutes, followed by 40 cycles of 95°C for 10 seconds, and 60°C for 1 minute. Primers are shown in Supplementary Table S2. Glyceraldehyde-3-phosphate dehydrogenase (*GAPDH*) served as an endogenous reference gene. The results are presented as ΔCt (Ct of the gene of interest – Ct of *GAPDH*). Smaller ΔCt values represent higher levels of gene expression. The fold changes in the expression of target genes also were calculated using the formula: RQ = 2 – ΔΔCt.

Statistical Analysis

SigmaPlot 11.0 (Systat Software, Inc., San Jose, CA, USA) was used for statistical analysis. Data are presented as the mean ± SEM. A 2-tailed Student's *t*-test or the Mann-Whitney *U* test were performed when comparing two groups. A P value < 0.05 was considered to be statistically significant.

Results

Light Injury Can Be Induced in C57BL/6J Mice After Intraperitoneal Fluorescein Injection

C57BL/6 mice are resistant to light injury in large part due to the Leu450Met variant in *RPE65*. Dyes like rose bengal and fluorescein[30,31] can increase the susceptibility of the retina to light injury. We hypothesized that different doses of fluorescein would allow us to induce retinal light damage with different levels of severity. C57BL/6J mice were exposed to light plus fluorescein as discussed in the methods. Compared to mice that were not exposed to light (Fig. 1A), 10 days after light exposure there was evidence of significant retinal injury on exam (Figs. 1B–E) and OCT (Figs. 1G–J). Meanwhile, eyes of mice injected with fluorescein but no light did not show any damage (Figs. 1A, 1F). C57BL/6J mice exposed to the same amount of light, but no fluorescein did not show any light injury (data not shown). Increasing the dose of fluorescein increased the severity of the injury. A separate experiment corroborated these findings in the higher fluorescein dose, and showed that the damage persisted up to 21 days after injury (Fig. 2). Interestingly, we found that increasing the interval between fluorescein injection and the start of the light stimulus (from 3 to 10 minutes) led to an increase in the level of injury. In the "Fl-4@3" model (4 minutes of 54 K lux light starting 3 minutes after the fluorescein injection) we consistently observed prominent RPE mottling (Figs. 2B, 2C) and thinning of the outer retinal layers in OCT (Figs. 2E, 2F). However, in the "Fl-4@10" model (4 minutes of 54 K lux light starting 10 minutes after the fluorescein injection) there was

Investigative Ophthalmology & Visual Science

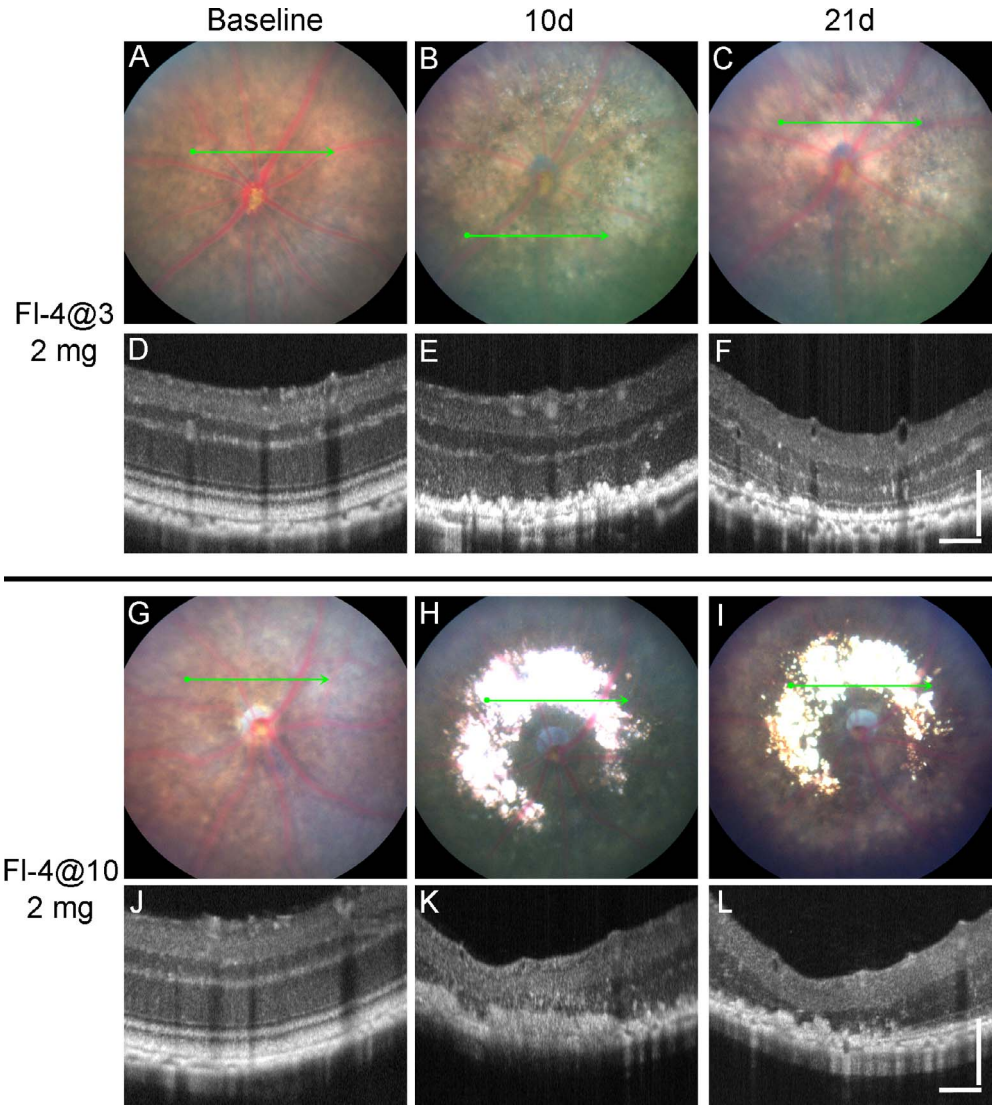

Figure 2. Fundus photos and OCT images from three time points in eyes exposed to the high dose of fluorescein and to the two light exposure protocols. Representative B6J eye at baseline (**A**, **D**), 10 days after (**B**, **E**), and 21 days after (**C**, **F**) exposure to 4 minutes of 54 K lux starting 3 minutes after the intraperitoneal injection of 2 mg fluorescein (Fl-4@3). Representative B6J eye at baseline (**G**, **J**), 10 days after (**H**, **K**), and 21 days after (**I**, **L**) exposure to 4 minutes of 54 K lux starting 10 minutes after the intraperitoneal injection of 2 mg fluorescein (Fl-4@10). *Optical coherence tomography scale bars*: 100 μm for *vertical* and *horizontal bars*.

prominent RPE atrophy on fundus photos (Figs. 2H, 2I) and severe destruction/disruption of the RPE and outer retina on OCT (Figs. 2K, 2L).

Light Injury Also Can Be Induced Without Fluorescein but Requires Higher Levels of Light

To demonstrate that light alone is sufficient to induce retinal toxicity in C57BL/6J mice we generated a model independent of fluorescein. We initially tried to use several light sources from dissecting microscopes (halogen or LED light) using intensities of up to 125,000 to 150,000 lux, but were not successful in obtaining retinal degeneration after up to 30 minutes of exposure (data not shown). Using the Micron III fundus camera we were able to induce retinal degeneration (Zhang K, et al. *IOVS* 2011;52:ARVO E-Abstract 977), but after upgrading to the Micron IV system we were unable to reproduce our results. We learned that one of the changes that were incorporated into the Micron IV system was meant to decrease the light output of the machine to increase safety. Phoenix Research Laboratories kindly agreed to remove the hardware aperture-lowering piece that reduced the light output for a small fee. This led to an increase in maximal output from 54 to 125 K lux. Using the maximum 125 K lux we were able to start seeing some level of light-induced degeneration after 20 minutes of direct exposure (data not shown). The toxicity was more consistent and significant after 30 minutes of light exposure (Figs. 3, 4). The retinal changes still were mild compared to those seen after intraperitoneal fluorescein. However, after 10 days, mild pigmentary changes could be seen in a circular area around the ONH corresponding to the area of light exposure (Fig. 3C). Furthermore, hyperreflectivity of the outer retinal layers could be seen after 3 and 10 days (Figs. 3E, 3F). These changes were not measured in the fluorescein-assisted model, since the more severe damage in that model led to prominent disruption/loss of the photore-

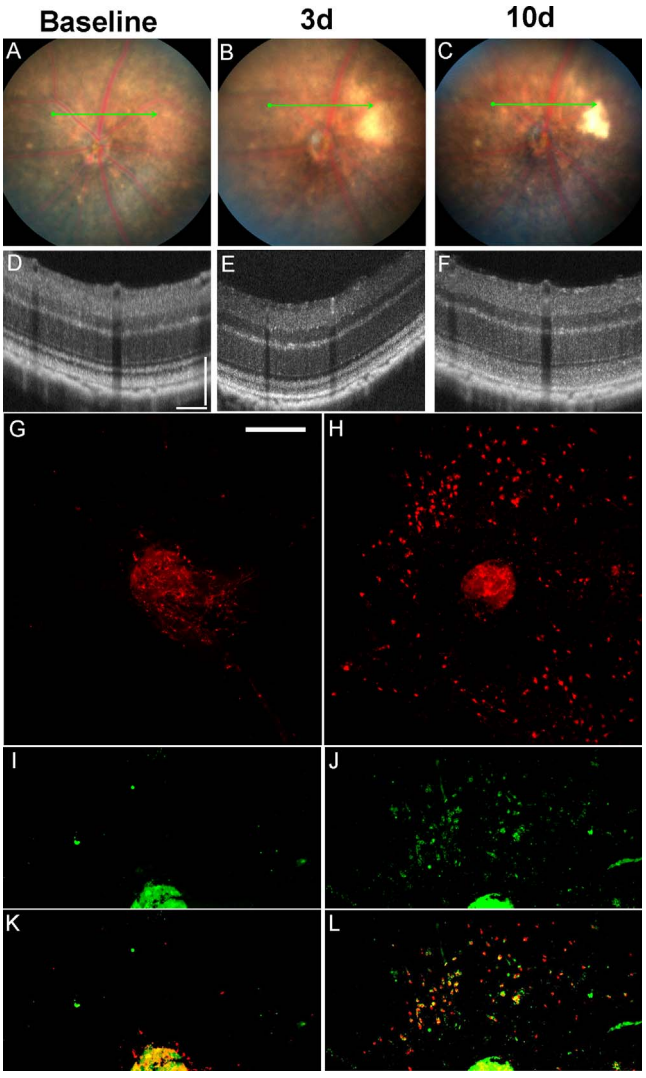

Figure 3. Fundus photos, OCT and RPE flat-mounts of eyes treated with a "Light-only" FCD-LIRD protocol. (**A**–**F**) Fundus photos and OCT images of a C57BL/6J eye at baseline (**A**, **D**) and also 3 d (**B**, **E**) and 10 d (**C**, **F**) after exposure to 125 K lux of white light for 30 minutes. (**G**–**L**) RPE flat-mounts of two C57BL/6J eyes stained with Iba-1 (**G**, **H**), CD16 (**I**, **J**), or merging of the two channels (**K**, **L**). *Left* corresponds to an untreated eye (**G**, **I**, **K**), while *right* (**H**, **J**, **L**) corresponds to an eye collected 8 days after treatment with 125 K lux of white light for 30 minutes using the FCD-LIRD protocol. *Optical coherence tomography scale bars*: 100 μm for *vertical* and *horizontal bars*. *Flat mount scale bar*: 250 μm.

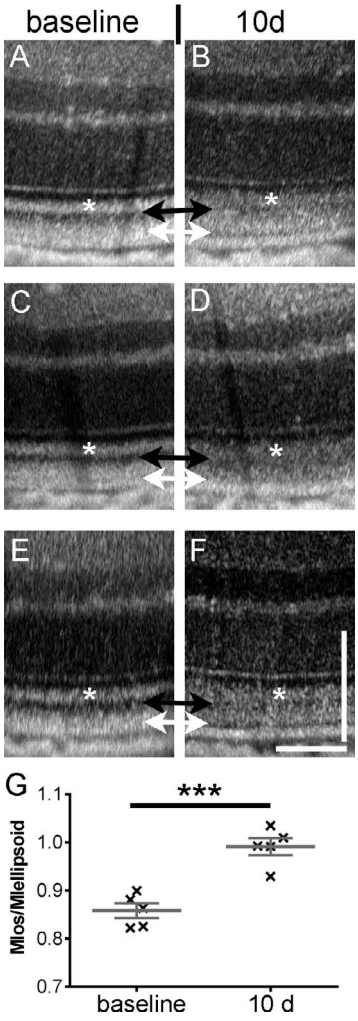

Figure 4. Optical coherence tomography images and reflectivity analysis before and after the "Light-only" FCD-LIRD protocol. Optical coherence tomography images of three different C57BL/6J eyes are shown before treatment (**A**, **C**, **E**) and 10 days after treatment (**B**, **D**, **F**) with 125 K lux for 30 minutes. The *black arrows* show increased reflectivity of the photoreceptor outer segments after light exposure. The *white arrows* show a new hyporeflective band just above the RPE after light exposure. There also is decreased reflectivity of the interdigitation zone (area between the *black* and *white arrows*) after light exposure. (**G**) Reflectivity analysis of the outer segments (*black arrows*) compared to the ellipsoid zone (*white asterisks*) in five C57BL/6J eyes before and after light exposure.

ceptor outer segments. Accumulation of Iba-1+ subretinal microglia could be seen in flat mounts 8 days after light injury (3H). Some of those cells also were positive for CD16+ (Figs. 3J, 3L). Subretinal microglia could be seen as early as 2 days after light injury (data not shown). Analysis of the OCT images 10 days after light injury without fluorescein revealed increased reflectivity of the photoreceptor outer segments (Fig. 4, black arrows), decreased reflectivity of the interdigitation zone (between the black and white arrows), and a new very thin hyporeflective band just above the RPE (Fig. 4, white arrows). Image J analysis of pixel intensity in the region of the outer segments (black arrows) and the ellipsoid zone (white asterisks) revealed that there was a statistically significant change after light injury compared to baseline (Fig. 4G).

Both Models of Fundus Camera Delivered (FCD)-LIRD Induce Measurable OCT Changes by Day 3

In BALB/c mice, thinning of the retina can be demonstrated consistently on OCT even 3 days after light damage.[32] Using FCD-LIRD on B6J mice, we also could see that by day 3 there was a statistically significant thinning of the outer nuclear layer (ONL; Fig. 5A), and also a decrease in "outer retinal thickness" (Fig. 5B; measured from the external limiting membrane to the bottom of the hyperreflective band that includes the RPE). This was true for the "Light-only" and the fluorescein models. Furthermore, the thinning was more prominent in the fluorescein model compared to the Light-only model ($P < 0.001$ for Fl-4@3 vs. "Light-only" and also for Fl-4@10 vs. "Light-only").

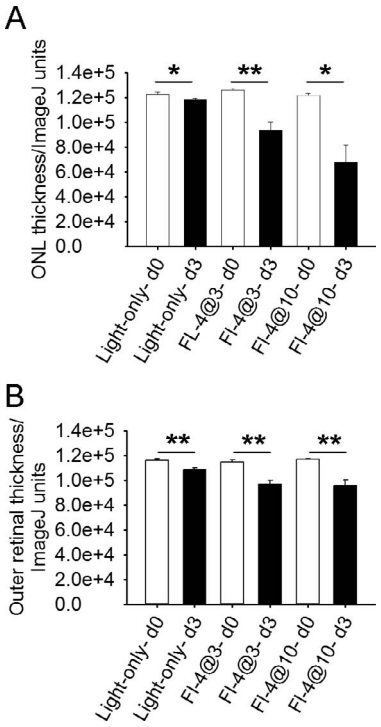

Figure 5. Quantitation of ONL and outer retina on OCT shows thinning after FCD-LIRD. (**A**) Optical coherence tomography ONL thickness measured in ImageJ units in C57BL/6J eyes before (d0) and 3 days after FCD-LIRD with either the "Light-only" protocol (125 K lux of light for 30 minutes, $n = 8$ eyes) or the fluorescein-assisted protocols (2 mg fluorescein followed by 4 minutes of 54 K lux of white light starting either 3 minutes after the injection ["Fl-4@3"], $n = 6$ eyes, or 10 minutes after the injection ["Fl-4@10"], $n = 5$ eyes). (**B**) Outer retinal thickness was also measured (bottom of Bruch's membrane to bottom of external limiting membrane) in the same eyes.

Apoptosis Is Involved in the Outer Retinal Thinning Seen After Light-Induced Retinal Degeneration

To better understand the anatomic changes caused by the different FCD-LIRD models we examined mouse eyes by histology 21 days after either the high intensity "Fl-4@10" fluorescein protocol or the "light-only" protocol (30 minutes of 125 K lux). A statistically-significant reduction in the thickness of the ONL was detected in both treatment groups when compared to no light exposure. It was mild in the "Light-only" protocol (Fig. 6B) and severe in the "Fl-4@10" protocol (Fig. 6C). Retinal pigment epithelium changes including RPE loss were seen in the "Light-only" model, and were even more pronounced in the "Fl-4@10" model (Figs. 6B, 6C). Subretinal debris, subretinal cells, and RPE hyperplasia also were noted in eyes treated with the more severe "Fl-4@10" protocol (Fig. 6C). Interestingly, the retinal thinning was statistically significant in a large area extending at least 800 μm from the optic nerve head in each direction (Fig. 6D). Similar to observations by others,[33,34] the superior retina was consistently the most sensitive to light injury. To eliminate the concern of a potential impact of tissue processing artifacts on our measurements, we corroborated our results by measuring the ONL as # of nuclei (Supplementary Fig. S1). These results closely parallel Figure 6D and confirm a statistically significant reduction in ONL thickness in both light injury models, which is greatest in the superior retina.

Since it is known that light injury in nonpigmented *RPE65*-450Leu mice causes retinal outer nuclear cell layer apoptosis, we wanted to determine if the FCD-LIRD model recapitulated this finding. Using a TUNEL assay, we found that 3 days after light exposure there was an increase in TUNEL+ cells mostly in the ONL in both light injury models. This increase was more pronounced in the "Fl-4@10" group (Fig. 6G) compared to the "Light-only" group (Fig. 6F). Quantification of the TUNEL+ cells revealed that the difference was statistically significant (data not shown): there was an average of 3.2 ± 1.1 cells in control eyes ($n = 4$), 26 ± 3 cells in the "Light-only" group ($n = 3$; $P < 0.05$ compared to control), and 194 ± 82 cells in the "Fl-4@10" group ($n = 3$; $P < 0.05$ compared to control).

Gene Expression Changes and Immunohistochemistry Confirm Light-Induced Oxidative Stress

Several groups have shown that light damage in nonpigmented mice can lead to gene-expression changes consistent with a response to oxidative stress.[19,35] To determine if the FCD-LIRD model induced oxidative stress, we isolated RNA from the posterior segment of eyes of B6J mice treated with the "Light-only" protocol and from age-matched naïve B6J mice. We first did a small preliminary experiment pooling cDNA from 2 to 4 treated versus untreated eyes and used a modified Qiagen "PCR Array for Mouse Oxidative Stress and Antioxidant Defense RT^2 profiler" to screen for oxidative stress genes (data not shown). We selected a few genes of interest for qPCR confirmation. RNA was isolated from eyes without light damage ($n = 8$ eyes), eyes 4 hours after the "Light-only" model of FCD-LIRD ($n = 6$ eyes; Fig. 7A; Supplementary Table S3), and eyes 24 hours after "Light-only" FCD-LIRD ($n = 4$ eyes; Fig. 7B; Supplementary Table S4). We found that 4 hours after light injury, while expression of *Nfe212* (gene for *Nrf2*) was not changed, there was a significant increase in *Stat3*, indicating that this oxidative-stress related pathway is triggered by light injury. Furthermore, there was a significant increase in multiple oxidative stress-related genes, including *Lpo*, *HO-1*, *Srnx1*, *Hspa1a* (*Hsp70*) and *Ptgs2* (*Cox-2*). Several of these genes (*Stat3*, *HO-1*, and *Srnx1*) were still significantly increased 24 hours after injury. It is important to note that *Nrf2* activity is more dependent on the speed of its degradation and its migration to the nucleus than on gene expression modulation. Thus, absence of *Nrf2* gene expression changes does not rule out *Nrf2* dysregulation after LIRD.[36]

Immunohistochemistry on eyes collected 3 days after light injury (using the "Fl-4@10" model) demonstrated that eyes after LIRD had an increased expression of the oxidative stress marker HO-1 (Fig. 7D) and also complement factor C3d (Fig. 7F).

Discussion

Light-induced retinal degeneration models have led to a great deal of knowledge regarding the retinal response to light injury. Hypoxia, hypoxia inducible factors, and erythropoietin,[37–39] halothane anesthesia,[40] complement inhibition (CFD KO mice),[17] iron chelation,[20] dexamethasone,[41] and free-radical scavengers[42] all can lead to decreased light injury. On the other hand, blue light may increase light injury[43] by promoting the regeneration of rhodopsin.[44] One proposed pathway for light-induced apoptosis starts by absorption of light energy by rhodopsin. In the presence of the Leu450 variant of *RPE65*, rhodopsin regenerates very quickly and becomes available for additional light absorption. The Met450 variant slows down rhodopsin regeneration and limits the

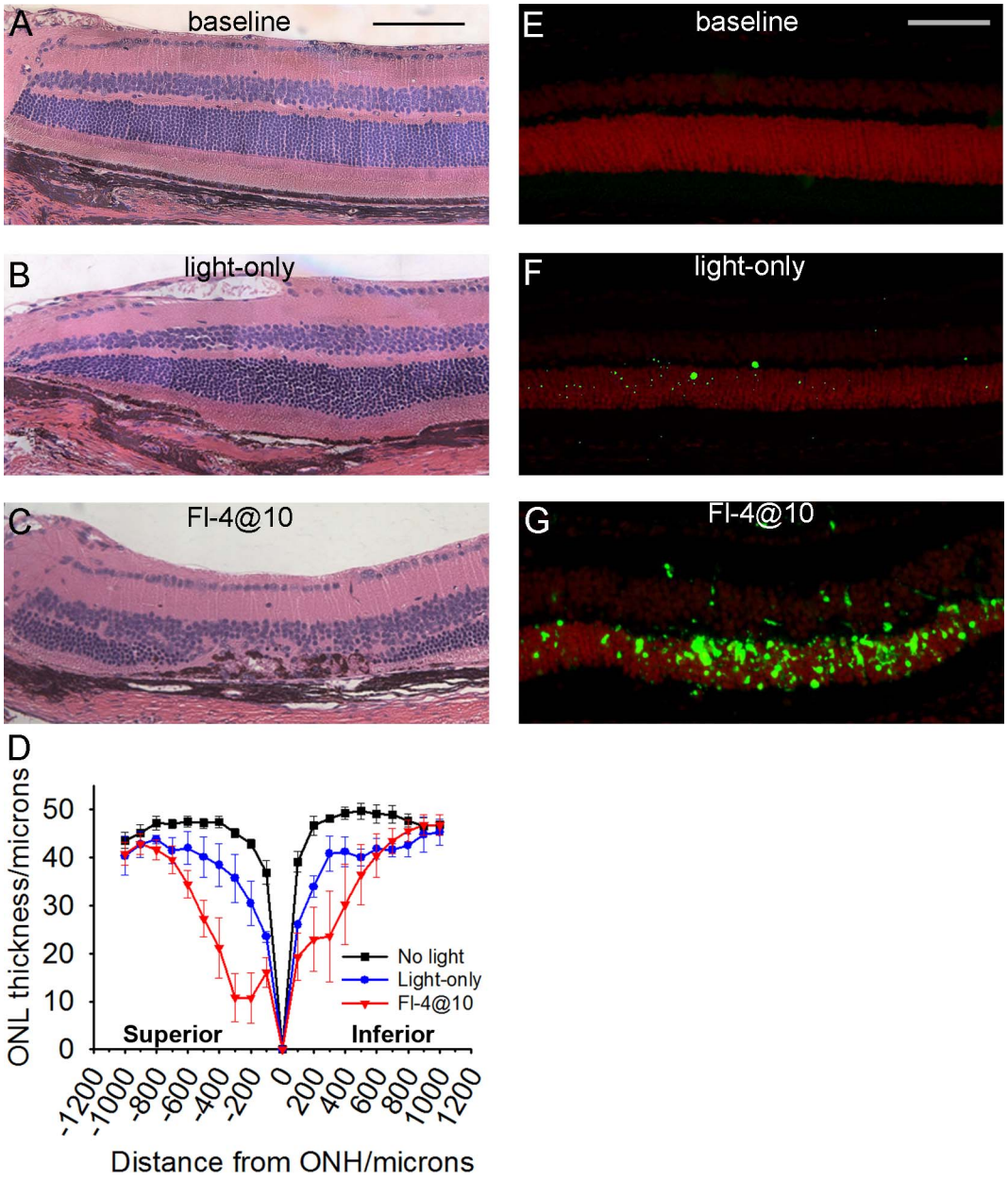

Figure 6. Retinal thinning and apoptosis after fundus camera-delivered light-induced retinal degeneration protocols. Histology images (**A**–**C**) and TUNEL staining (**E**–**G**) in C57BL/6J eyes that were either naive (**A**, **E**), exposed to the "Light-only" FCD-LIRD protocol (30 minutes of 125 K lux of white light; [**B**, **F**]), or exposed to the fluorescein-assisted protocol ("Fl-4@10"; 2 mg of fluorescein followed 10 minutes later by 54 K lux; [**C**, **G**]). Eyes for histology were collected 21 days after treatment. Eyes for TUNEL staining were collected 3 days after treatment. (**D**) Outer nuclear thickness was measured on histology sections at 100-µm intervals in eyes without treatment ($n = 5$), 21 days after "Light-only" FCD-LIRD ($n = 3$), and 21 days after Fl-4@10 light ($n = 5$). *Scale bars*: (**A**) 100 µm, (**E**) 75 µm.

amount of light energy absorption in the retina. Light-induced photoreceptor cell death may involve the interplay of multiple pathways, including ER stress, NF kappa B/caspase-1 activation, and autophagy.[45–47]

Importantly, little is known about the response of the retina to light exposure in the setting of resistance to light damage. It is clear that the human retina is much more resistant to light damage than that of albino rodents. To address this issue, we developed a rapid and reproducible model of light damage that is applicable to mouse strains that are relatively resistant to light damage. The FCD-LIRD model uses the Micron IV fundus camera to deliver light to the retina. The light source is a broad spectrum Xenon light source, filtered so that the spectrum is limited to between 450 and 680 nm (within the visible light spectrum) for ocular safety. It should be noted that the Micron IV system did not induce any heat damage to the cornea or iris. We have not seen any anterior segment injuries in over 200 mice that have been treated in our laboratory with the FCD-LIRD model. We incorporated the use of fluorescein based on prior studies showing that it increases the susceptibility of the retina to light injury.[30,31] The settings used for the fluorescein-assisted models demonstrated that this model allows for the titration of the retinal degeneration along a very wide spectrum of severities. It is likely that intensities lower than 54 K lux may still allow for significant FCD-LIRD. Although the mechanism for the fluorescein-related increase in susceptibility to light

Investigative Ophthalmology & Visual Science

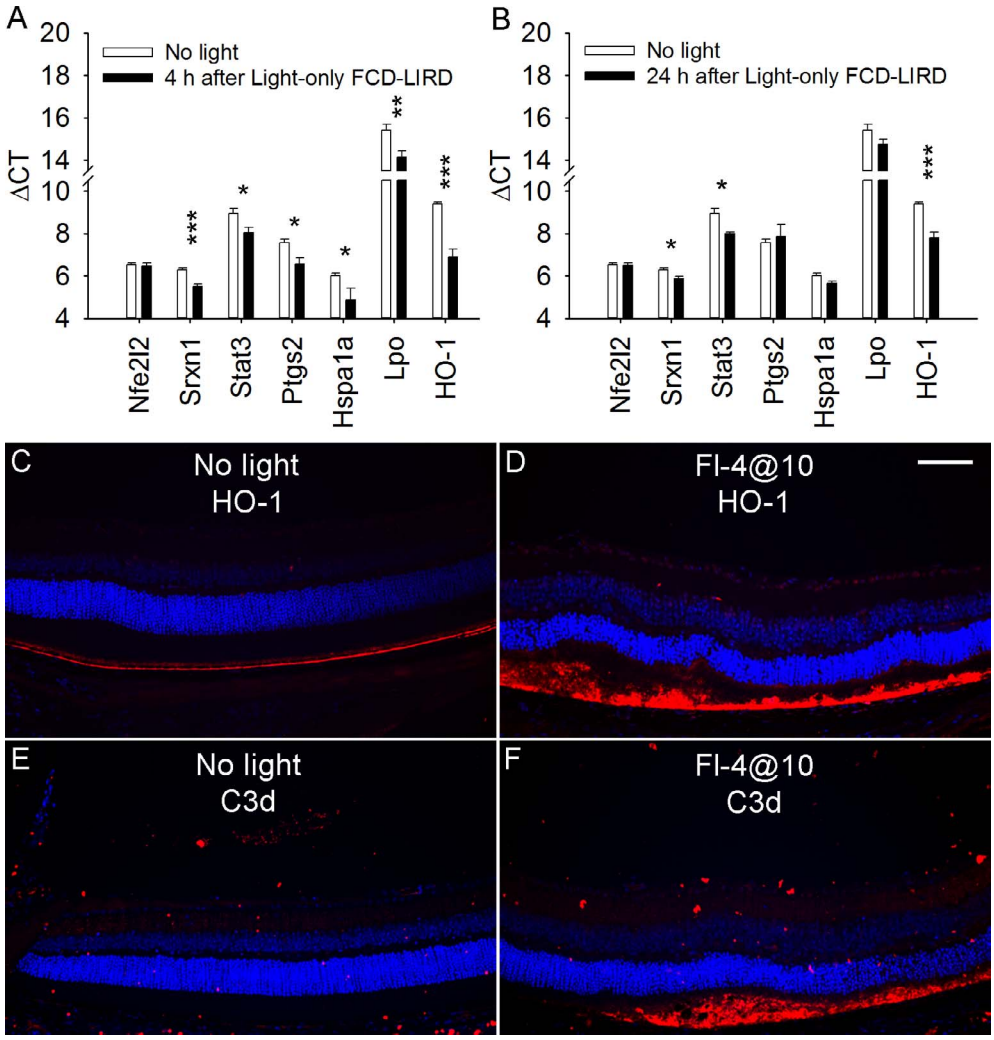

Figure 7. Oxidative stress-related gene and protein expression after FCD-LIRD. RNA was isolated from eyes without light damage ($n = 8$ eyes), 4 hours after "Light-only" (30 minutes of 125 K lux) FCD-LIRD ($n = 6$ eyes) and 24 hours after "Light-only" FCD-LIRD ($n = 4$ eyes). Values for ΔCT ($Ct_{PROBE} - Ct_{GAPDH}$) are shown for eyes collected at 4 (**A**) or 24 (**B**) hours after light exposure. A *smaller bar* indicates a higher level of gene expression. Gene expression changes were determined using the formula: $RQ = 2 - \Delta\Delta Ct$ (Supplementary Tables S3, S4). Immunohistochemistry of retinal sections from naïve (**C**, **E**) or light exposed (**D**, **F**) C57BL/6J mice demonstrates increased HO-1 (**D**) and C3d (**F**) staining after light damage using 2 mg of intraperitoneal fluorescein followed 10 minutes later by 4 minutes of illumination with 54 K lux of white light ("FI-4@10"). *Scale bar*: (**D**) 75 μm.

damage is not understood, it is interesting that the damage still starts at the photoreceptor/outer-retina level. In the Light-only protocol, we did not see significant damage with intensities lower than 125K lux or durations lower than 20 minutes. We tried to use the fluorescein angiography filter of the Micron IV system to deliver blue light. However, perhaps due to the lower light intensity, we found lower levels of retinal degeneration. We did not observe choroidal neovascularization (CNV) in either one of the LIRD models. Of the over 200 mice to which we have applied the FCD-LIRD model, we have looked at over 100 eyes 2 to 4 weeks after FCD-LIRD and have not found any evidence of CNV on fundus photos, OCT, fluorescein angiography (FA) or retinal sections (data not shown).

Despite very careful coupling of the Micron IV camera and the mouse eye to ensure excellent centration of the eye and avoid oblique illumination, we consistently found that the superior retina was more sensitive to FCD-LIRD than the inferior retina. This was consistent with reports in other models[33,34] and suggested that our model is mediated by rhodopsin light absorption, since rod outer segment length and retinal axial absorbance in the rodent retina is known to be higher in the superior retina.[48] Although there still is some debate, the increased susceptibility of the superior retina to light injury may be due to the phenomenon of photostasis,[48] which may be the result of an accommodation of the retina to the distribution of light exposure chronically. In other words, because on a regular basis the superior rodent retina receives less light than the inferior retina, it compensates in ways that increase its sensitivity to light, making it also more susceptible to light damage.

The FCD-LIRD model has several advantages: it allows for the reproducible induction of retinal injury in pigmented mice carrying the *RPE65*-Met450 variant; it can be titrated to generate a wide range of levels of retinal degeneration; it reproduces many of the findings seen in other models of retinal degeneration, including the rhodopsin-driven sensitivity of the superior retina, the apoptosis of the ONL, and the recruitment

Investigative Ophthalmology & Visual Science

of subretinal microglia/macrophages; it is associated with the induction of an oxidative-stress response and seems to be exacerbated in mice deficient in oxidative-stress response enzymes (data not shown); the amount of light delivered is not dependent on factors like mouse eye closure, or light blockage due to mouse position or interference by bedding or other objects; and it can be used to deliver the same amount of light to a fairly large number of mice over a short period of time, making it a feasible option for moderately-high-throughput studies. Disadvantages of our model include the need for a minor modification to the Micron camera (at least for the "Light-only" model), and the need for an experienced operator that can ensure consistent eye-camera coupling. Another caveat of our study is that for some of the experiments we included low numbers of mice, as for example, in the TUNEL assay. We should note that the increase in TUNEL+ cells in FCD-LIRD–treated eyes was pronounced, and statistical significance could be reached with just 3 to 4 eyes per group.

From the histology measurements (Fig. 6D) it is clear that the FCD-LIRD model generates retinal changes over a large area. Since OCT sections provide only data on a slice of tissue, one of our goals is to find an outcome measure that determines the effect of the light damage over a large area of retina. Possible parameters would include volumetric OCT analysis, and automated analysis of ZO-1 staining of RPE flat-mounts.[49,50]

Acknowledgments

Supported by National Institutes of Health (NIH; Bethesda, MD, USA) Grant 1R01EY022652, Visual Science Core Grant EY020799, an unrestricted grant from Research to Prevent Blindness, the Patricia and Col. William Massad Retina Research Fund, and a grant from the David M. Crowley Foundation.

Disclosure: **X. Zhong**, None; **B. Aredo**, None; **Y. Ding**, None; **K. Zhang**, None; **C.X. Zhao**, None; R**.L. Ufret-Vincenty**, None

References

1. Weismann D, Hartvigsen K, Lauer N, et al. Complement factor H binds malondialdehyde epitopes and protects from oxidative stress. *Nature*. 2011;5;478:76–81.
2. Hollyfield JG, Bonilha VL, Rayborn ME, et al. Oxidative damage-induced inflammation initiates age-related macular degeneration. *Nat Med*. 2008;14:194–198.
3. Brantley MA Jr, Osborn MP, Sanders BJ, et al. Plasma biomarkers of oxidative stress and genetic variants in age-related macular degeneration. *Am J Ophthalmol*. 2012;153: 460–467.
4. Ding X, Patel M, Chan CC. Molecular pathology of age-related macular degeneration. *Prog Retin Eye Res*. 2009;28:1–18.
5. Shaw PX, Zhang L, Zhang M, et al. Complement factor H genotypes impact risk of age- related macular degeneration by interaction with oxidized phospholipids. *Proc Natl Acad Sci U S A*. 2012;109:13757–13762.
6. Rohrer B, Bandyopadhyay M, Beeson C. Reduced metabolic capacity in aged primary retinal pigment epithelium (RPE) is correlated with increased susceptibility to oxidative stress. *Adv Exp Med Biol*. 2016;854:793–798.
7. Shen JK, Dong A, Hackett SF, Bell WR, Green WR, Campochiaro PA. Oxidative damage in age-related macular degeneration. *Histol Histopathol*. 2007;22:1301–1308.
8. Zhao Z, Chen Y, Wang J, et al. Age-related retinopathy in NRF2-deficient mice. *PLoS One*. 2011;6:e19456.
9. Punzo C, Xiong W, Cepko CL. Loss of daylight vision in retinal degeneration: are oxidative stress and metabolic dysregulation to blame? *J Biol Chem*. 2012;287:1642–1648.
10. Campochiaro PA, Strauss RW, Lu L, et al. Is there excess oxidative stress and damage in eyes of patients with retinitis pigmentosa? *Antioxid Redox Signal*. 2015;23:643–648.
11. Komeima K, Rogers BS, Lu L, Campochiaro PA. Antioxidants reduce cone cell death in a model of retinitis pigmentosa. *Proc Natl Acad Sci U S A*. 2006;103:11300–11305.
12. Delcourt C, Cougnard-Grégoire A, Boniol M, et al. Lifetime exposure to ambient ultraviolet radiation and the risk for cataract extraction and age-related macular degeneration: the Alienor Study. *Invest Ophthalmol Vis Sci*. 2014;55:7619–7627.
13. Tomany SC, Cruickshanks KJ, Klein R, Klein BE, Knudtson MD. Sunlight and the 10-year incidence of age-related maculopathy: the Beaver Dam Eye Study. *Arch Ophthalmol*. 2004;122:750–757.
14. Paskowitz DM, LaVail MM, Duncan JL. Light and inherited retinal degeneration. *Br J Ophthalmol*. 2006;90:1060–1066.
15. White DA, Fritz JJ, Hauswirth WW, Kaushal S, Lewin AS. Increased sensitivity to light- induced damage in a mouse model of autosomal dominant retinal disease. *Invest Ophthalmol Vis Sci*. 2007;48:1942–1951.
16. Wenzel A, Grimm C, Samardzija M, Remé CE. Molecular mechanisms of light-induced photoreceptor apoptosis and neuroprotection for retinal degeneration. *Prog Retin Eye Res*. 2005;24:275–306.
17. Rohrer B, Guo Y, Kunchithapautham K, Gilkeson GS. Eliminating complement factor D reduces photoreceptor susceptibility to light-induced damage. *Invest Ophthalmol Vis Sci*. 2007;48:5282–5289.
18. Joly S, Francke M, Ulbricht E, et al. Cooperative phagocytes: resident microglia and bone marrow immigrants remove dead photoreceptors in retinal lesions. *Am J Pathol*. 2009;174: 2310–2323.
19. Hadziahmetovic M, Kumar U, Song Y, et al. Microarray analysis of murine retinal light damage reveals changes in iron regulatory, complement and antioxidant genes in the neurosensory retina and isolated RPE. *Invest Ophthalmol Vis Sci*. 2012;53:5231–5241.
20. Song D, Song Y, Hadziahmetovic M, Zhong Y, Dunaief JL. Systemic administration of the iron chelator deferiprone protects against light-induced photoreceptor degeneration in the mouse retina. *Free Radic Biol Med*. 2012;53:64–71.
21. O'Koren EG, Mathew R, Saban DR. Fate mapping reveals that microglia and recruited monocyte-derived macrophages are definitively distinguishable by phenotype in the retina. *Sci Rep*. 2016;6:20636.
22. Zheng L, Anderson RE, Agbaga MP, Rucker EB III, Le YZ. Loss of BCL-XL in rod photoreceptors: increased susceptibility to bright light stress. *Invest Ophthalmol Vis Sci*. 2006;47:5583–5589.
23. Wenzel A, Reme CE, Williams TP, Hafezi F, Grimm C. The Rpe65 Leu450Met variation increases retinal resistance against light-induced degeneration by slowing rhodopsin regeneration. *J Neurosci*. 2001;21:53–58.
24. Wenzel A, Grimm C, Samardzija M, Remé CE. The genetic modifier Rpe65Leu(450): effect on light damage susceptibility in c-Fos-deficient mice. *Invest Ophthalmol Vis Sci*. 2003;44: 2798–2802.
25. Grimm C, Remé CE. Light damage as a model of retinal degeneration. *Methods Mol Biol*. 2013;935:87–97.
26. Luhmann UF, Robbie S, Munro PM, et al. The drusenlike phenotype in aging Ccl2-knockout mice is caused by an accelerated accumulation of swollen autofluorescent subretinal macrophages. *Invest Ophthalmol Vis Sci*. 2009;50:5934–5943.
27. Mattapallil MJ, Wawrousek EF, Chan CC, et al. The Rd8 mutation of the Crb1 gene is present in vendor lines of C57BL/6N mice and embryonic stem cells and confounds ocular

induced mutant phenotypes. *Invest Ophthalmol Vis Sci*. 2012; 53:2921–2927.

28. Ufret-Vincenty RL, Aredo B, Liu X, et al. Transgenic mice expressing variants of complement factor H develop AMD-like retinal findings. *Invest Ophthalmol Vis Sci*. 2010;51:5878–5887.
29. Aredo B, Zhang K, Chen X, Wang CX, Li T, Ufret-Vincenty RL. Differences in the distribution, phenotype and gene expression of subretinal microglia/macrophages in C57BL/6N (Crb1 rd8/rd8) versus C57BL6/J (Crb1 wt/wt) mice. *J Neuroinflammation*. 2015;12:6.
30. Hochheimer BF, D'Anna SA, Calkins JL. Retinal damage from light. *Am J Ophthalmol*. 1979;88:1039–1044.
31. Hunter JJ, Morgan JI, Merigan WH, Sliney DH, Sparrow JR, Williams DR. The susceptibility of the retina to photochemical damage from visible light. *Prog Retin Eye Res*. 2012;31:28–42.
32. Aziz MK, Ni A, Esserman DA, Chavala SH. Evidence of early ultrastructural photoreceptor abnormalities in light-induced retinal degeneration using spectral domain optical coherence tomography. *Br J Ophthalmol*. 2014;98:984–989.
33. Rapp LM, Williams TP. A parametric study of retinal light damage in albino and pigmented rats. In: Williams TP, Baker BN. eds. *The Effects of Constant Light on Visual Processes*. New York: Springer US Press; 1980:135–159.
34. Rapp LM, Smith SC. Morphologic comparisons between rhodopsin-mediated and short- wavelength classes of retinal light damage. *Invest Ophthalmol Vis Sci*. 1992;33:3367–3377.
35. Grimm C, Wenzel A, Hafezi F, Remé CE. Gene expression in the mouse retina: the effect of damaging light. *Mol Vis*. 2000;6: 252–260.
36. Harder B, Jiang T, Wu T, et al. Molecular mechanisms of Nrf2 regulation and how these influence chemical modulation for disease intervention. *Biochem Soc Trans*. 2015;43:680–686.
37. Grimm C, Wenzel A, Groszer M, et al. HIF-1-induced erythropoietin in the hypoxic retina protects against light-induced retinal degeneration. *Nat Med*. 2002;8:718–724.
38. Lange C, Heynen SR, Tanimoto N, et al. Normoxic activation of hypoxia-inducible factors in photoreceptors provides transient protection against light-induced retinal degeneration. *Invest Ophthalmol Vis Sci*. 2011;528:5872–5880.
39. Chung H, Lee H, Lamoke F, Hrushesky WJ, Wood PA, Jahng WJ. Neuroprotective role of erythropoietin by antiapoptosis in the retina. *J Neurosci Res*. 2009;87:2365–2374.
40. Keller C, Grimm C, Wenzel A, Hafezi F, Remé C. Protective effect of halothane anesthesia on retinal light damage: inhibition of metabolic rhodopsin regeneration. *Invest Ophthalmol Vis Sci*. 2001;42:476–480.
41. Wenzel A, Grimm C, Seeliger MW, et al. Prevention of photoreceptor apoptosis by activation of the glucocorticoid receptor. *Invest Ophthalmol Vis Sci*. 2001;42:1653–1659.
42. Mitra RN, Merwin MJ, Han Z, Conley SM, Al-Ubaidi MR, Naash MI. Yttrium oxide nanoparticles prevent photoreceptor death in a light-damage model of retinal degeneration. *Free Radic Biol Med*. 2014;75:140–148.
43. Collier RJ, Wang Y, Smith SS, et al. Complement deposition and microglial activation in the outer retina in light-induced retinopathy: inhibition by a 5-HT1A agonist. *Invest Ophthalmol Vis Sci*. 2011;52:8108–8116.
44. Grimm C, Wenzel A, Williams T, Rol P, Hafezi F, Remé C. Rhodopsin-mediated blue-light damage to the rat retina: effect of photoreversal of bleaching. *Invest Ophthalmol Vis Sci*. 2001;42:497–505.
45. Chen Y, Sawada O, Kohno H, et al. Autophagy protects the retina from light-induced degeneration. *J Biol Chem*. 2013; 288:7506–7518.
46. Yang LP, Wu LM, Guo XJ, Li Y, Tso MO. Endoplasmic reticulum stress is activated in light-induced retinal degeneration. *J Neurosci Res*. 2008;86:910–919.
47. Wu T, Chiang SK, Chau FY, Tso MO. Light-induced photoreceptor degeneration may involve the NF kappa B/caspase-1 pathway in vivo. *Brain Res*. 2003;967:19–26.
48. Penn JS, Williams TP. Photostasis: regulation of daily photon-catch by rat retinas in response to various cyclic illuminances. *Exp Eye Res*. 1986;43:915–928.
49. Chalfoun J, Majurski M, Dima A, Stuelten C, Peskin A, Brady M. FogBank: a single cell segmentation across multiple cell lines and image modalities. *BMC Bioinformatics*. 2014;15:431.
50. Bray MA, Vokes MS, Carpenter AE. Using CellProfiler for automatic identification and measurement of biological objects in images. *Curr Protoc Mol Bio*l. 2015;109:1–13.

Investigative Ophthalmology & Visual Science